HTRA1 (High Temperature Requirement A Serine Peptidase 1) Gene Is Transcriptionally Regulated by Insertion/Deletion Nucleotides Located at the 3′ End of the ARMS2 (Age-related Maculopathy Susceptibility 2) Gene in Patients with Age-related Macular Degeneration*

Daisuke Iejima[‡], Takeshi Itabashi[‡], Yuich Kawamura[‡], Toru Noda[§], Shinsuke Yuasa[¶], Keiichi Fukuda[¶], Chio Oka[‖], and Takeshi Iwata[‡1]

From the [‡]Division of Molecular and Cellular Biology, National Institute of Sensory Organs, and the [§]Division of Ophthalmology, National Hospital Organization Tokyo Medical Center, Tokyo 152-8902, Japan, the [¶]Department of Cardiology, Keio University School of Medicine, Tokyo 160-8582, Japan, and the [‖]Division of Gene Function in Animals, Nara Institute of Science and Technology, Nara 630-0101, Japan

Background: The biological function of insertion/deletion sequences associated with AMD has not been fully characterized.
Results: The HTRA1 regulatory region contains an insertion/deletion sequence that is significantly up-regulated in retinal neuronal cell lines.
Conclusion: HTRA1 expression is enhanced by a mutation in the insertion/deletion in the HTRA1 regulatory region.
Significance: This is the characterization of the HTRA1 regulatory elements and the effect of insertion/deletion sequences associated with AMD.

Dry age-related macular degeneration (AMD) accounts for over 85% of AMD cases in the United States, whereas Japanese AMD patients predominantly progress to wet AMD or polypoidal choroidal vasculopathy. Recent genome-wide association studies have revealed a strong association between AMD and an insertion/deletion sequence between the ARMS2 (age-related maculopathy susceptibility 2) and HTRA1 (high temperature requirement A serine peptidase 1) genes. Transcription regulator activity was localized in mouse retinas using heterozygous HtrA1 knock-out mice in which HtrA1 exon 1 was replaced with β-galactosidase cDNA, thereby resulting in dominant expression of the photoreceptors. The insertion/deletion sequence significantly induced HTRA1 transcription regulator activity in photoreceptor cell lines but not in retinal pigmented epithelium or other cell types. A deletion construct of the HTRA1 regulatory region indicated that potential transcriptional suppressors and activators surround the insertion/deletion sequence. Ten double-stranded DNA probes for this region were designed, three of which interacted with nuclear extracts from 661W cells in EMSA. Liquid chromatography-mass spectrometry (LC-MS/MS) of these EMSA bands subsequently identified a protein that bound the insertion/deletion sequence, LYRIC (lysine-rich CEACAM1 co-isolated) protein. In addition, induced pluripotent stem cells from wet AMD patients carrying the insertion/deletion sequence showed significant up-regulation of the HTRA1 transcript compared with controls. These data suggest that the insertion/deletion sequence alters the suppressor and activator cis-elements of HTRA1 and triggers sustained up-regulation of HTRA1. These results are consistent with a transgenic mouse model that ubiquitously overexpresses HtrA1 and exhibits characteristics similar to those of wet AMD patients.

Recent genome-wide association studies have identified more than 19 susceptibility genes associated with age-related macular degeneration (AMD)[2] (1). Among these genes, two loci have been highly associated with AMD, and these include the CFH (complement factor H) gene on chromosome 1q32 and the ARMS2/HTRA1 (age-related macular degeneration susceptibility 2/high temperature requirement A1) gene on chromosome 10q26. Although a strong association of CFH Y402H (rs1061170) with Caucasians with dry AMD has been established (2, 3), this locus has not been associated with the majority of Japanese patients with wet AMD (4). Rather, ARMS2/HTRA1 is the region most strongly associated with wet AMD in Japanese patients (5, 6). Moreover, the single nucleotide polymorphism (SNP), rs10490924, was shown in a single linkage disequilibrium (LD) block to increase the risk of wet AMD in both Caucasian and Japanese AMD populations (6). This LD block included the entire ARMS2 gene and a portion of HTRA1 exon 1 (Fig. 1). However, genome-wide association studies alone are insufficient to distinguish between these two candidate genes. Previous reports have identified an insertion/deletion region ~443 bp in length that immediately follows the

2 The abbreviations used are: AMD, age-related macular degeneration; LD, linkage disequilibrium; RPE, retinal pigment epithelium; PCV, polypoidal choroidal vasculopathy; iPSC, induced pluripotent stem cell; TLR, Toll-like receptor.

second exon of *ARMS2* within the regulatory element of *HTRA1* (7, 8). This finding led to confusion as to whether a single gene or both *ARMS2* and *HTRA1* are involved in AMD. *ARMS2* is a recent gene evolutionarily and is within the primate lineage (7, 9). Its protein product, ARMS2, has been shown to localize to the mitochondria of the inner segment of the photoreceptor (7) and to interact with fibulin-6 in the extracellular matrix of the choroid (10). However, details regarding the biological function(s) of ARMS2 remain unclear (7, 9, 10). In contrast, *HTRA1* has been characterized to some extent. HTRA1 belongs to the HTRA serine protease family, which is highly conserved from microorganisms to multicellular organisms, including humans (11). Several cellular and molecular studies have suggested that HTRA1 plays a key role in regulating various cellular processes via the cleavage and/or binding of pivotal factors that participate in cell proliferation, migration, and cell fate (12–15). Recently, up-regulation of human *HTRA1* expression in the mouse retinal pigment epithelium (RPE) was shown to induce a branching network of choroidal vessels and polypoidal lesions and severe degeneration of the elastic lamina and tunica media of the choroidal vessels, similar to that observed in AMD and PCV patients (16, 17). A mutation in *HTRA1* has also been associated with a hereditary form of familial cerebral small vessel disease (CARASIL (cerebral autosomal recessive arteriopathy with subcortical infarcts and leukoencephalopathy)) (18). The original report by Dewan *et al.* (19) described the up-regulation of HTRA1 in fibroblasts obtained from AMD patients. This result was both confirmed and denied by several other groups and was also subjected to a regulatory element characterization assay containing the insertion/deletion sequence (7, 8). However, the results obtained were based on transcription regulator activity that was measured using the human RPE cell line, ARPE19. On the basis of previous study, the purpose of this study is to characterize transcription regulation of *ARMS2 and HTRA1* genes in wet form AMD.

EXPERIMENTAL PROCEDURES

Subjects—A total of 226 Japanese patients with typical wet AMD without PCV (average age, 74.68 ± 8.86 years) were classified as 5b according to Seddon *et al.* (20). In addition, 228 non-AMD Japanese individuals (average age, 75.22 ± 7.23 years) were recruited as controls for this study (Table 1). All patients were diagnosed by fundus observation or by fluorescein/indocyanine green angiographic findings. For the controls, no signs of early AMD, such as soft drusen or alterations of the retinal pigment epithelium in the macula area, were observed ophthalmoscopically. Informed consent was obtained from all of the patients and controls, and the procedures performed conformed to the tenets of the Declaration of Helsinki.

DNA Isolation and Sequencing—Human DNA was extracted from blood samples using a Magtration System 8Lx (Precision System Science Co., Ltd., Tokyo, Japan). The *PLEKHA1-ARMS2-HTRA1* region of genomic DNA was amplified from both control and AMD patient samples using the primers listed in Table 1. PCR amplifications for all primer sets were performed in a 20-μl volume containing 100 ng of genomic DNA and 1 unit of *Taq* polymerase (PrimerStar, Takara Bio Co. Ltd., Japan) for 35–40 cycles of amplification. Amplified PCR products were then

TABLE 1
Primers used for sequencing

Primer name	Sequence
PLEKHA1-ARMS2-F1	CCCCATGCTTTCAGGGTTCACC
PLEKHA1-ARMS2-R1	GGGGTCTCATTCTGTTGTCCAGGC
PLEKHA1-ARMS2-F2	TGTTCCCAGCCTCTCCCCACTCTT
PLEKHA1-ARMS2-R2	GAACCACTTCTCCCAGCCAAACACT
PLEKHA1-ARMS2-F3	GTTCAGTGGCGCAATCTCGGC
PLEKHA1-ARMS2-R3	CCTCATGCACTGCTAGTGGGATTGT
PLEKHA1-ARMS2-F4	CAGGCTGGAGTGCAATGGTGTGAT
PLEKHA1-ARMS2-R4	GGAGGATTGCTTGAGCCCAGGAC
PLEKHA1-ARMS2-F5	CTACGTGGCGGGCGCTGTCT
PLEKHA1-ARMS2-R5	CTGTGTTGGCTGGACTCGGTAGCT
ARMS2-F1	CTGAGCCGAGGAGTATGAGG
ARMS2-R1	CAGGAACCACCGAGGAGGACAGAC
ARMS2-F2	TCCCTGAGACCACCCAACAA
ARMS2-R2	CGCGCTCACATTTAGAACAT
ARMS2-F3	GCGCTTTGTGCTTGCCATAGT
ARMS2-R3	CCAAAATAGGACAAAGGTGAGG
ARMS2-F4	GTGAAACCCCATCTCTACTAAAAATACAG
ARMS2-R4	CCCACATCAGTTCAGTTAGGTTCGGTTCAG
ARMS2-F5	GCTTGGCAGTCACATGTAGTTAGT
ARMS2-R5	CAGGCCTTGGCACGGTATTCT
ARMS2-HTRA1-F2	CAAGGCCTGGTGAGTGAGAAATGAGTT
ARMS2-HTRA1-R2	GAGGGGGTGGAGAATGGGTAAGAGG
ARMS2-HTRA1-F3	TCCACTTCGGCCGACACTTCCTC
ARMS2-HTRA1-R3	TGCCTTTCTTTGCCCACATCTCC
ARMS2-HTRA1-F4	TGGGGGCACGAGGATGGAAGAG
ARMS2-HTRA1-R4	AGGGAATGAGCGGACCGAAAACAGT
ARMS2-HTRA1-F5	TGGGCAAAGAAAGGCACAGAGACC
ARMS2-HTRA1-R5	TGGGGCAGATGGAATTAAAAGGACA
ARMS2-HTRA1-F6	CCGCAAAGCAGTGGGGAAGTT
ARMS2-HTRA1-R6	CCTCATCCCGAACCCTCAAACCTC
ARMS2-HTRA1-F7	TTGAGGGGGCTTATAGGTATTTGGAGTT
ARMS2-HTRA1-R7	GGGTGGCATGCGTGTCCGTATTC
ARMS2-HTRA1-F8	CCCAACGGATGCACCAAAGATTC
ARMS2-HTRA1-R8	CCCGGTCACGCGCTGGTTCT
ARMS2-HTRA1-F9	ACGCATGCCACCCACAACAACTTTT
ARMS2-HTRA1-R9	GCGGGATCTGCATGGCGACTCT

purified using an ExoSAP-IT kit (GE Healthcare) and were sequenced using a BigDye Terminator version 3.1 sequencing kit (Invitrogen) and an ABI 3130 Genetic Analyzer.

Cell Culture—The mouse photoreceptor cell line, 661W, and the rat retinal ganglion cell line, RGC5, were cultured in Dulbecco's modified Eagle's medium (DMEM) containing 10% fetal bovine serum (FBS) at 37 °C in 5% CO_2. The human RPE cell line, ARPE19, was cultured in DMEM/F-12 containing 15% FBS at 37 °C in 5% CO_2.

Transcription Regulator Activity Assay—The *ARMS2* regulatory region and the *HTRA1* regulatory region were amplified and cloned into the pGL4.10 (Luc2) luciferase vector (Promega, WI) (Table 2). Insertion/deletion variants were also constructed using a KOD mutagenesis kit (Toyobo, Osaka, Japan). For the luciferase assays performed, 661W cells, RGC5 cells, and ARPE19 cells were seeded in 96-well plates (1×10^4 cells/well) 24 h before transfection. Transfections were performed using Lipofectamine LTX with Plus reagent (Invitrogen). A firefly luciferase gene was integrated into a reporter vector to normalize the activity of both transcription regulators. Luciferase activity was detected using the Dual-Glo luciferase assay system (Promega) and a microplate reader (Plate Chameleon, Hidex, Turku, Finland).

Preparation of Induced Pluripotent Stem Cells (iPSCs) from Controls and AMD Patients—Human iPSCs were established by infecting circulating T cells obtained from the peripheral blood of human AMD patients with the Sendai virus as described previously (21, 22). Briefly, peripheral blood mononuclear cells were obtained from donors by the centrifugation

Characterization of HTRA1 Regulatory Elements

TABLE 2
Primer used for cloning

Number	Oligonucleotide sequence[a]	Forward/Reverse	Enzyme site	Description	Type
1	ACGT**CTCGAG**GCCTCGCAGCGGTGACGAG	Reverse	XhoI	Reverse primer	Normal, in/del
2	ACGT**GAGCTC**AGATGCAGCCCAATCTTCTCCTAACA	Forward	SacI	Normal or in/del: full-length	Normal, in/del
3	ACGT**GAGCTC**CCCTCCTTTCTCTCCCGGGTG	Forward	SacI	Normal or in/del: Δ82	Normal, in/del
4	ACGT**GAGCTC**TGTCTAGCAGTGTCTACCCTGTGGCA	Forward	SacI	Normal: Δ298	Normal
5	ACGT**GAGCTC**GGTGTACCTGCTGTTAAAGGAGGT	Forward	SacI	Normal: Δ384	Normal
6	ACGT**GAGCTC**AATGGGTGAGTAGGGATGGATTACA	Forward	SacI	Normal: Δ543	Normal
7	ACGT**GAGCTC**AATGGGTGAGTAGGGATGGATTA	Forward	SacI	In/del: Δ148	In/del
8	AATGGGTGAGTAGGGATGGATTACACC	Inverse-F		In/del: Δin/del-F	In/del
9	CCGGGAGAGAAAGGAGGGCAA	Inverse-R		In/del: Δin/del-R	In/del

[a] Boldface sequence, restriction enzyme site for cloning.

TABLE 3
EMSA probe sequence

Number	Type	Probe sequence
1	Sense	AGATGCAGCCCAATCTTCTCCTAACATCTGGATTCCTCTC
	Antisense	GAGAGGAATCCAGATGTTAGGAGAAGATTGGGCTGCATCT
2	Sense	GATTCCTCTCTGTCACTGCATTCCCTCCTGTCATCCTGCC
	Antisense	GGCAGGATGACAGGAGGGAATGCAGTGACAGAGAGGAATC
3	Sense	TCATCCTGCCTTTGTTTTCTTGCCCTCCTTTCTCTCCCGG
	Antisense	CCGGGAGAGAAAGGAGGGCAAGAAAACAAAGGCAGGATGA
4	Sense	GGTGTACCTGCTGTTAAAGGAGGTTACGACCTCTGATGCT
	Antisense	AGCATCAGAGGTCGTAACCTCCTTTAACAGCAGGTACACC
5	Sense	ATGCTGGGGTGGCCAGAGGGGATGGGAGTGGGTCTGGCAC
	Antisense	GTGCCAGACCCACTCCCATCCCCTCTGGCCACCCCAGCAT
6	Sense	GGCACTCTGAGGAAAGGGGGTGAAACCAGCTGAGAAGTCA
	Antisense	TGACTTCTCAGCTGGTTTCACCCCCTTTCCTCAGAGTGCC
7	Sense	AGTCATCTTTTACCTGCTGGCATGGCCCCAGCCAGGGTTC
	Antisense	GAACCCTGGCTGGGGCCATGCCAGCAGGTAAAAGATGACT
8	Sense	CCCCAGCCAGGGTTCTGTTGCTATGGGAGAATGGGTGAGT
	Antisense	ACTCACCCATTCTCCCATAGCAACAGAACCCTGGCTGGGG
9	Sense	TCTCTCCCGGTTATTAATTAATTAACTAAAATTAAATTAT
	Antisense	ATAATTTAATTTTAGTTAATTAATAACCGGGAGAGA
10	Sense	AATTATTTAGTTAATTTAATTAACTAAACTAATGGGTGAG
	Antisense	CTCACCCATTAGTTTAGTTAATTAAATTAACTAAATAATT

of heparinized blood over a Ficoll-Paque PREMIUM (GE Healthcare) gradient, according to the manufacturer's instructions. The peripheral blood mononuclear cells were then cultured at 37 °C in 5% CO_2 with plate-bound anti-CD3 monoclonal antibodies (BD Pharmingen) in GT-T502 medium (Kohjin Bio, Sakado, Japan) supplemented with recombinant interleukin-2 (IL-2) at 175 Japan reference units/ml. After 5 days, activated peripheral blood mononuclear cells were collected and transferred to 6-well plates (1.5×10^6 cells/well) coated with anti-CD3 monoclonal antibodies, and the cells were incubated for an additional 24 h. A solution containing Sendai virus vectors that individually carried OCT3/4, SOX2, KLF4, and c-MYC (DNAVEC Inc., Japan) was added to each well. At 24 h postinfection, the medium was changed to fresh CT-T502 medium. At 48 h postinfection, the cells were collected and transferred to a 10-cm dish that contained mitomycin C-inactivated mouse embryonic fibroblast feeder cells (6×10^4 to 6×10^5 cells/dish). After an additional 24 h of incubation, the medium was changed to iPSC medium, which consisted of DMEM/F-12 medium (Sigma) supplemented with 20% knockout serum replacement (Invitrogen), 1 mM L-glutamine, 1 mM non-essential amino acids, 0.1 mM β-mercaptoethanol, 50 units of penicillin, 50 mg/ml streptomycin, and 4 ng/ml basic fibroblast growth factor (Wako Pure Chemical Industries, Osaka, Japan). The iPSC medium was changed every other day until colonies were picked. The generated iPSCs were maintained on irradiated mouse embryonic fibroblast feeder cells in iPSC medium. Culture medium for the iPSCs was changed every 2 days, and the cells were passaged using 1 mg/ml collagenase IV every 5–6 days.

EMSA—Nuclear extracts were prepared with a CelLytic nuclear extraction kit (Sigma), according to the manufacturer's protocol. The nuclear protein concentration of each sample was determined using a BCA protein assay kit (Thermo Scientific).

EMSA probes were 40 bp in length and are listed in Table 3. Probes 1–3 were designed to cover non-insertion/deletion and insertion/deletion regions (non-insertion/deletion, bp −4320 to −4220; insertion/deletion, bp −3936 to −3836). Probes 4–8 were designed to cover the non-insertion/deletion regulatory region (non-insertion/deletion, bp −3936 to −3777). Probes 9 and 10 were designed to cover the insertion/deletion region (insertion/deletion, −3836 to −3782 bp). Double-stranded DNA probes were biotin-labeled using a LightShift chemiluminescent EMSA kit (Thermo Scientific) and then were mixed with nuclear extracts. After 20 min, the samples were subjected to electrophoresis on 7% EMSA gels. After electrophoresis, the samples were transferred onto Biodyne B precut modified nylon membranes (Thermo Scientific). The membranes were cross-linked in a UV transilluminator for 15 min and then were incubated with blocking buffer and streptavidin-horseradish peroxidase conjugates. Bound conjugates were detected using a molecular imager (ChemiDoc XRS+, Bio-Rad).

RT-PCR—The iPSCs were removed from the feeder cells and were rinsed twice with PBS. Total cellular RNA was extracted with TRIzol reagent (Invitrogen), according to the manufactur-

er's instructions. RNA concentrations were determined by measuring absorption values at 260 nm/280 nm. Reverse transcription was performed using a SuperScript first strand synthesis system for RT-PCR kit (Invitrogen). Primer sequences for human *OCT3/4*, *NANOG*, *SOX2*, and *GAPDH* as well as the associated PCR detection methods were created and performed according to Seki *et al.* (21). The primers used to detect human *HTRA1* included AACTTTATCGCGGACGTGGTGGAG (forward) and TGATGGCGTCGGTCTGGATGTAGT (reverse).

Quantitative RT-PCR—Total RNA was isolated from human iPSCs with an RNeasy minikit (Qiagen, Hilden, Germany) according to the manufacturer's instructions. An aliquot of each sample was reverse-transcribed using a high capacity cDNA reverse transcription kit (Invitrogen) to obtain single-stranded cDNAs. Using an ABI STEP-One real-time PCR system (Invitrogen) with TaqMan probes for human *HTRA1*, quantitative RT-PCR was performed according to the manufacturer's instructions. All of the reactions were run in triplicate using the ΔCt method, and detection of human *GAPDH* was used as an internal control.

Liquid Chromatography-Mass Spectrometry (LC-MS/MS)—Nuclear extract of 661W cells (50 μg) was combined with 100 pmol of biotin-labeled, double-stranded DNA probes in DNAP buffer (20 mM HEPES, 80 mM KCl, 1 mM MgCl, 0.2 mM EDTA, 10% glycerol, 0.1% Triton X-100, 0.5 mM DTT). This proteins/probes mixture was incubated at 4 °C for 30 min before 50 ml of Dynabeads M280 streptavidin (Invitrogen) was added. The mixture was incubated at 4 °C for 30 min. The beads-probes-protein complex was then washed with 500 μl of DNAP buffer three times for 30 min at 4 °C. The washed complexes were mixed with 30 μl of SDS-PAGE sample buffer (Bio-Rad) and were boiled for 5 min at 100 °C. The boiled samples were quenched on ice for 5 min before being separated by 7.5% SDS-PAGE. Bands of interest were cut out of the gel and were processed for in-gel digestion for further LC-MS/MS analysis. A Thermo LTQ system (Thermo Scientific) and Scaffold 4 data analysis software (Matrix Science) were used.

Immunohistochemistry—Eyes from wild type, *HtrA1* knock-out, and *HtrA1* transgenic mice (12, 16, 23) were resected and immersed in a fixative containing 4% paraformaldehyde overnight at 4 °C. The eyes were embedded in OCT compound and frozen on dry ice. Sections of the frozen eyes (10 μm) were washed with 0.1% Tween 20, PBS (PBST) prior to permeabilization with 0.3% Triton X-100, PBS for 15 min. After the sections were washed in 0.1% PBST, they were incubated with blocking solution for 1 h, followed by an overnight incubation at 4 °C with anti-rabbit HtrA1 antibodies (Abcam) in PBS, 2% BSA. The sections were washed in 0.1% PBST three times and then were incubated with Alexa Fluor 488-conjugated anti-rabbit IgG antibodies (1:1000; Invitrogen) and DAPI (Dojindo, Japan) for nuclear staining at room temperature. After 1 h, the sections were mounted with Ultramount aqueous permanent mounting medium (DakoCytomation, Glostrup, Denmark) and were analyzed using a confocal fluorescence laser microscope (LSM 700, Zeiss).

In Situ Hybridization—Eyes from *HtrA1* heterozygous mice were removed and immersed in 5% formaldehyde overnight at 4 °C. The eyes were then embedded in paraffin and sectioned

(10 μm). *In situ* hybridization was performed using a Quanti-Gene^{TM} ViewRNA system (Affymetrix, Santa Clara, CA) using HtrA1 and LacZ probes according to the manufacturer's instructions.

Western Blotting—Total proteins were extracted from mouse brain tissues in ice-cold TNE buffer (10 mM Tris-HCl, 100 mM NaCl, 10 mM EDTA, 0.1% Nonidet P-40) containing protease and phosphatase inhibitors (Roche Applied Science). Protein concentrations of the extracts were determined using a BCA assay kit (Thermo Scientific). Equal amounts of protein (10 μg/lane) were separated by 7.5% SDS-PAGE and were transferred to PVDF membranes (Trans-Blot Turbo, Bio-Rad). The membranes were then incubated with an anti-mouse HtrA1 antibody (1:100; Abcam) and an anti-α-tubulin antibody (1:1000; Abcam). A FluorChem Western blot imaging station (ChemiDoc XRS+, Bio-Rad) and image analysis software (Image Lab, Bio-Rad) were used to calculate and normalize the pixel value of each protein band.

RESULTS

Sequencing of ARMS2-HTRA1 Loci in Controls and AMD Patients—To determine the genomic sequence of the LD block represented by the SNP, rs10490924, in association with AMD (6, 19, 24), ~10.5 kbp of the LD block (NC_000010.10) was sequenced for 228 controls and 226 AMD patients. Two unique sequences were identified in the regulatory region of *ARMS2* and *HTRA1* (Fig. 1). A C-to-A (C/A) variant was identified in the regulatory region of *ARMS2*, −550 bp upstream of exon 1 (Fig. 1, *A* and *B*), and an insertion/deletion variant was identified immediately following the *ARMS2* exon 2 in the regulatory region of *HTRA1*, −3777 bp upstream of exon 1 (Fig. 1, *A* and *C*). Sequence variations in both transcription regulators were in complete LD with SNP rs10490924, thereby suggesting that AMD and PCV pathogenesis are directly associated with these variants.

The Effect of C/A and Insertion/Deletion Variants on ARMS2 and HTRA1 Regulatory Region Activity—To date, two hypotheses have been proposed to account for the increased risk of AMD that is observed. These involve an increase in the transcription of *HTRA1* and/or the presence of unstable *ARMS2* mRNA (7, 19, 24). To investigate the first hypothesis, regulator activity for *ARMS2* was assayed using constructs covering the regulatory region from −1,000 to +1 bp and from −600 to +1 bp. Both of these regions contain the C/A repetitive variant (Fig. 1*D*). Regulatory region activity was not detected for either the non-C/A or C/A variants of differing length for retinal cell lines (ARPE19, 661W, and RGC5 tested) (Fig. 1, *E*–*G*). Next, regulator activity of *HTRA1* was assayed for the −4,320 to +1 bp region of the non-insertion/deletion regulatory region and for the −3,936 to +1 bp region of the insertion/deletion regulatory region (Fig. 1*H*). Both regions had common sequences on both ends of the regulatory region. Transcription regulator activity was not found to be affected by the insertion/deletion variants in the ARPE19 cell line (Fig. 1*I*). However, activity of the insertion/deletion regulator was significantly up-regulated compared with the activity of the non-insertion/deletion regulator in both the 661W and RGC5 cell lines, by ~2- and 3-fold, respectively (Fig. 1, *J* and *K*). Moreover, *HTRA1* non-insertion/
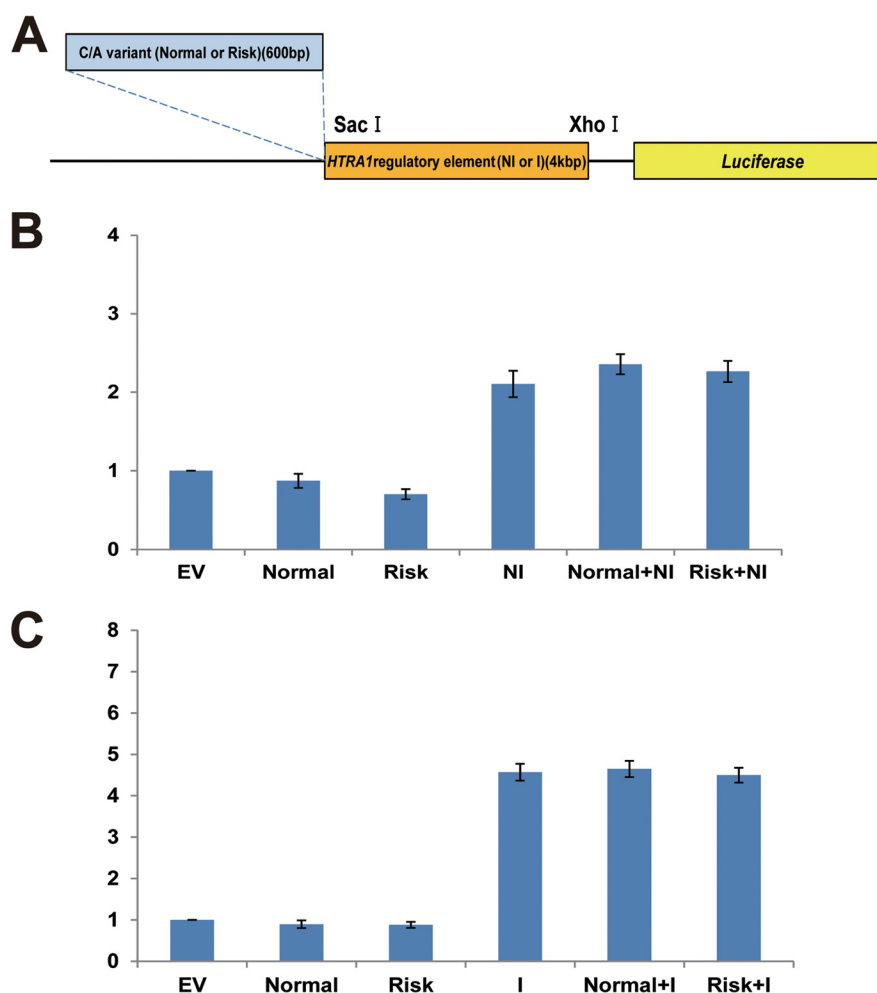
FIGURE 2. **The effect of the *ARMS2* C/A variant on the *HTRA1* transcription regulator.** *A*, schematic diagram of the C/A variant plus *HTRA1* regulatory element in the constructs used for luciferase assays (*blue region*, 600-bp *AMRS2* transcription regulatory region (contains C/A variant); *orange region*, region that contains the *HTRA1* regulatory element; *yellow region*, the luciferase reporter gene). *B*, C/A variant plus non-insertion/deletion type *HTRA1* regulatory element activity in 661W cells. *C*, C/A variant plus insertion/deletion type *HTRA1* regulatory element activity in 661W cells. *Error bars*, S.D. *EV*, empty vector; *Normal*, normal type C/A variant; *Risk*, risk type C/A variant; *NI*, non-insertion/deletion type *HTRA1* regulatory element; *I*, insertion/deletion type *HTRA1* regulatory element.

deletion regulator activity was not detected in the latter, similar to the empty vector. However, when the non-insertion/deletion regulator was replaced with the insertion/deletion regulator in the 661W and RGC5 cell lines, *HTRA1* regulatory element activity increased 2- and 3-fold, respectively (Fig. 1*J*). To test whether C/A variants in the transcription regulatory region of *ARMS2* influence *HTRA1* gene expression, both normal and risk type *ARMS2* C/A variant (Fig. 2*A*) were cloned and fused to the *HTRA1* transcription regulator of the non-insertion/deletion and insertion/deletion constructs. Luciferase levels were

subsequently measured following transfection of these vectors (Fig. 2*A*). Neither the normal nor the risk type, C/A variants affected *HTRA1* transcription regulator activity (Fig. 2, *B* and *C*).

Endogenous Transcription Regulator Activity and Protein and mRNA Expression of HtrA1 in Mouse Retina Tissues—To examine the localization of HtrA1 in the retina, eye sections from both wild type and mutant (HtrA1 knock-out, HtrA1 transgenic) mice were stained with an anti-mouse HtrA1 antibody (Fig. 3*A*). In both wild type and HtrA1-Tg mouse sections,

FIGURE 1. **Transcription regulatory region of *ARMS2* and *HTRA1*.** *A*, a schematic diagram of the transcription regulatory region of *ARMS2* and *HTRA1*. Sequencing of the indicated transcription regulatory region spanned 10.5 kbp and was performed for both AMD and non-AMD controls. Two unique sequences, a C/A repeat variant in the *ARMS2* transcription regulator (indicated with a *blue box*) and an insertion/deletion variant downstream of exon 2 of *ARMS2* (indicated with a *red box*), were identified in a patient with AMD that carried the SNP, rs10490924. *B*, characteristic C/A mutations present in the *ARMS2* transcription regulatory region (*blue*, C/A variant; *red*, C to A substitution). *C*, the insertion/deletion mutations present in the *HTRA1* transcription regulatory region (*blue*, ARMS2 exon 2 region; *red*, point mutations). *D–G*, analysis of *ARMS2* transcription regulator activity using a luciferase assay system. *D*, four luciferase vectors were generated to analyze *ARMS2* transcription regulator activity: normal (1,000 bp), normal (600 bp), risk (1,000 bp), and risk (600 bp). The 1,000-bp sequence contained a C/T SNP in the upper 730-bp region from *ARMS2* exon 1. *ARMS2* transcription regulator activity detected in ARPE19 cells (*E*), RGC-5 cells (*F*), and 661W cells (*G*). *Error bars*, S.D. *H–K*, *HTRA1* transcription regulator activity detected in various retinal cell lines. *H*, schematic diagram of the *ARMS2-HTRA1* constructs used in the luciferase assays performed (*black line*, common regulator sequence; *blue line*, non-insertion/deletion regulator unique sequence; *red line*, insertion/deletion regulator unique sequence). Full-length *HTRA1* transcription regulator activity detected in ARPE19 cells (*I*), RGC5 cells (*, $p = 7.5 \times 10^{-6}$) (*J*), and 661W cells (**, $p = 1.07 \times 10^{-6}$) (*K*). *Error bars*, S.D. *EV*, empty vector; *NI*, non-insertion/deletion regulator; *I*, insertion/deletion regulator.
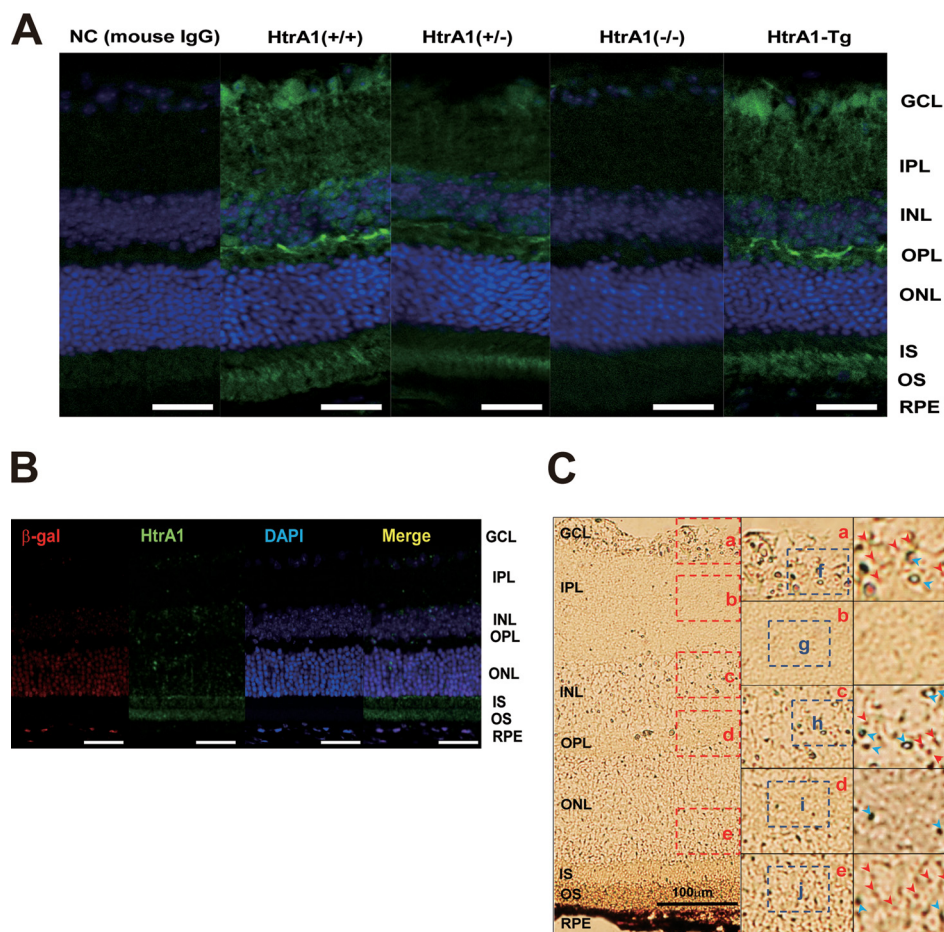
FIGURE 3. *Htra1 transcription regulator activity and Htra1 protein expression in the mouse retina. A,* immunohistochemistry to detect HtrA1 expression in $HtrA1^{+/+}$, $HtrA1^{+/-}$, $HtrA1^{-/-}$, and *HtrA1-Tg* mouse retinas (*blue,* DAPI; *green,* HtrA1). *NC* (mouse IgG), staining control; *scale bars,* 100 μm. *B,* immunohisto-chemistry to detect HtrA1 expression in $HtrA1^{+/-}$ mouse retinas (*red,* β-galactosidase; *green:* HtrA1; *blue,* DAPI; *yellow,* merge). *Scale bars,* 100 μm. *C, in situ* hybridization to detect *HtrA1* expression in $HtrA1^{+/-}$ mouse retina tissues (*red arrowheads,* HtrA1; *blue arrowheads,* β-galactosidase). *Scale bars,* 100 μM. *OS,* outer segment; *IS,* inner segment; *ONL,* outer nuclear layer; *OPL,* outer plexiform layer; *INL,* inner nuclear layer; *IPL,* inner plexiform layer; *GCL,* ganglion cell layer.

HtrA1 expression was observed to localize to the photore-ceptor cell layer (outer segment (*OS*) and inner segment (*IS*) in Fig. 3), the outer plexiform layer (*OPL*), and the ganglion cell layer (*GCL*). In contrast, HtrA1 expression in eye tissues from heterozygous *HtrA1* mice was mainly localized to the photoreceptor cell layer and the outer plexiform layer, whereas minor expression of HtrA1 was observed in the gan-glion cell layer.

To localize *HtrA1* transcription regulator activity in the ret-ina, a heterozygous *HtrA1* knock-out mouse construct that included β-galactosidase (β-gal) cDNA (*LacZ*) in place of exon 1 of *Htra1* was used. β-Gal protein was abundantly expressed in the outer nuclear layer (*ONL*), and lower levels of expression were observed in the RPE, the inner nuclear layer (*INL*), and the retinal ganglion cell layer (*GCL*) (Fig. 3*B*). In comparison, native HtrA1 protein was abundantly expressed in the OS and IS, with lower expression levels detected in the RPE, the outer plexiform layer (*OPL*), the inner plexiform layer (*IPL*), and the ganglion cell layer (Fig. 2*B*). Furthermore, abundant transcription of *HtrA1* mRNA was detected by *in situ* hybridization in retinal sections from a *HtrA1* heterozygous knock-out mouse (Fig. 3*C*). Taken together, these results suggest that *HtrA1* is tran-scribed mainly in the outer nuclear layer, outer plexiform layer,

and ganglion cell layer, and then the protein product is trans-ported to the photoreceptor layer.

Identification of Suppressing and Activating cis-Elements in the HTRA1 Regulatory Element—To analyze the mechanism of insertion/deletion function in the *HTRA1* regulatory region, both non-insertion/deletion (*1,* bp $-4,320$ to $+1$; *2,* bp $-4,238$ to $+1$; *3,* bp $-4,022$ to $+1$; *4,* bp $-3,936$ to $+1$; *5,* bp $-3,777$ to $+1$) and insertion/deletion (*6,* bp $-3,936$ to $+1$; *7,* bp $-3,854$ to $+1$; *8,* bp $-3,788$ to $+1$; *9,* bp $-3,836$ to $-3,788$ defect mutant) regions were cloned into a pGL4.10[*luc2*] luciferase assay vec-tor (Fig. 4*A*). These cloned vectors were then transfected into 661W cells and were analyzed for *HTRA1* transcription regula-tor activity. The activity of the number 2 region (bp $-4,320$ to $-4,239$) non-insertion/deletion defect *HTRA1* transcription regulator was 1.8–2-fold higher than that of the number 1 region, and transcription regulator activity did not differ between the number 2, 3, and 4 variants (Fig. 4*B*). In con-trast, the activity of the number 5 transcription regulator was 20–30% higher than that of the number 4 variant (Fig. 4*B*).

In addition, activity of the number 6 insertion/deletion type *HTRA1* transcription regulator was 2- and 3-fold higher than that of the number 1 non-insertion/deletion type transcription regulator in 661W cells (Figs. 1*K* and 4*C*). Furthermore, activity

A

Non-insertion/deletion type *HTRA1* regulatory elements

B

insertion/deletion type *HTRA1* regulatory elements
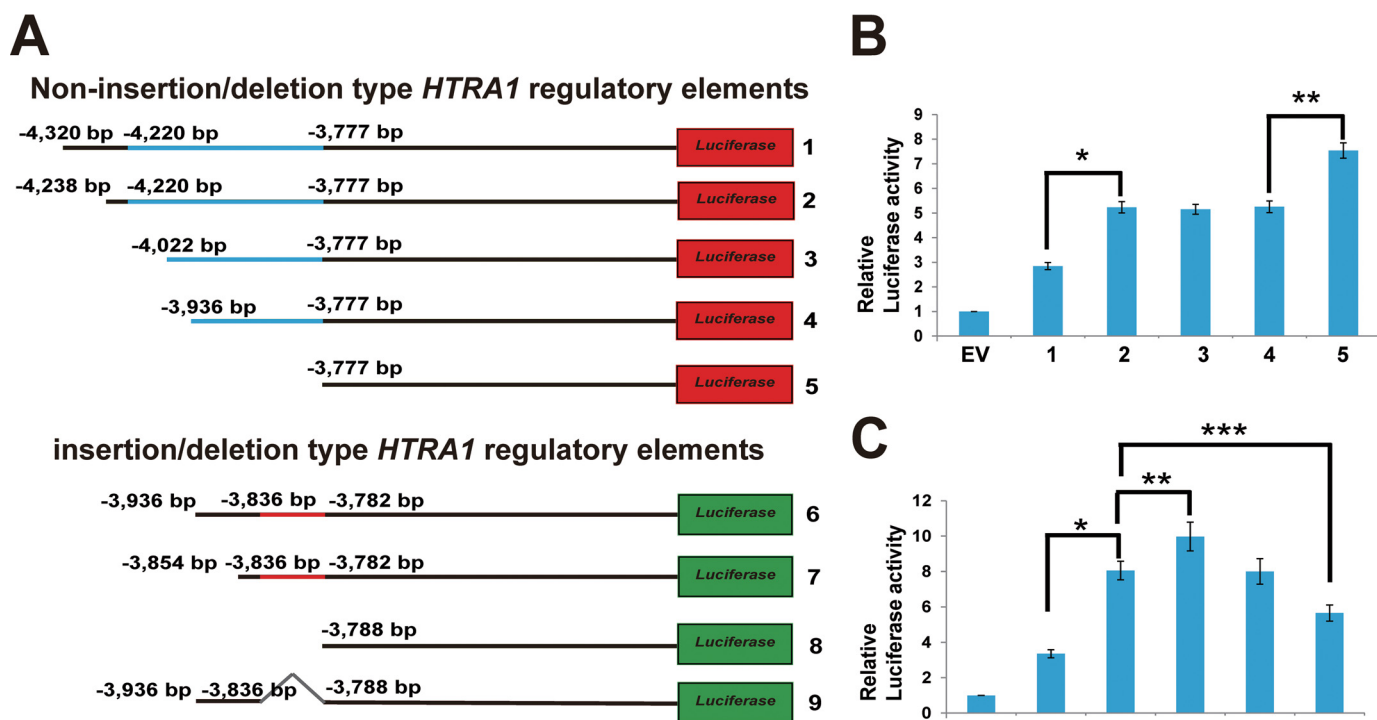

C

FIGURE 4. **Enhanced *HTRA1* transcription regulator activity is associated with the insertion/deletion variant in the photoreceptor cell line, 661W.** *A*, constructs used for luciferase assay analysis (*black line*, common sequence between both regulators; *blue line*, non-insertion/deletion regulator (443 bp); *red line*, insertion/deletion regulator (54 bp); *red boxes 1–5*, non-insertion/deletion regulator constructs; *green boxes 6–9*, insertion/deletion regulator constructs; *gray line 9*, insertion/deletion region). *B* and *C*, transcription regulator activity detected for the non-insertion/deletion and insertion/deletion *HTRA1* transcription regulator assayed (in *B*, *, $p = 1.05 \times 10^{-6}$; **, $p = 3.46 \times 10^{-5}$; in *C*, *, $p = 2.2 \times 10^{-6}$; **, $p = 0.0086$; ***, $p = 0.0062$). *EV*, empty vector; *error bars*, S.D.
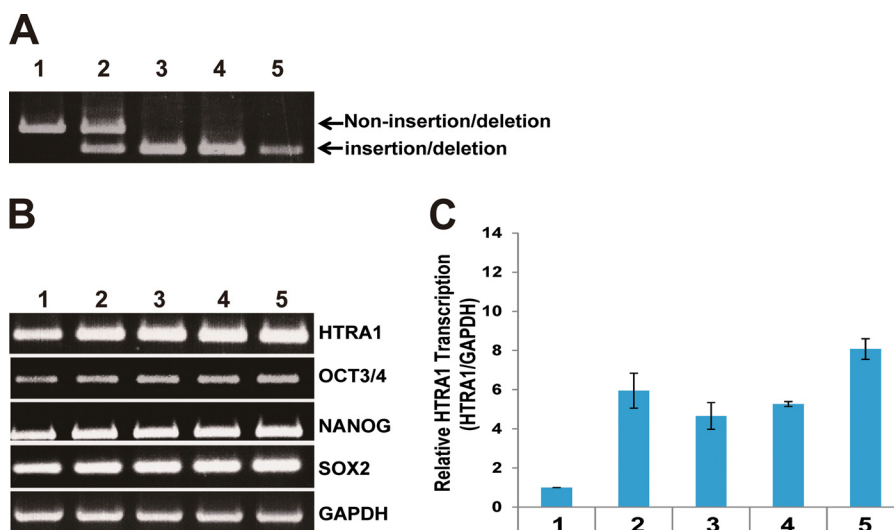
A

B

C

FIGURE 5. **HTRA1 transcription in human iPSCs derived from wet AMD patients.** *A*, genotyping of non-insertion/deletion *versus* insertion/deletion versions of the human *HTRA1* gene transcription regulatory region. *B*, detection of human iPSC marker genes by RT-PCR. Detection of GAPDH was used as an internal control. *C*, relative transcriptional level of *HTRA1* determined by quantitative RT-PCR for iPSCs derived from individuals with non-insertion/deletion (control) *versus* insertion/deletion (wet AMD) transcription regulators. *Sample 1*, 30-year-old non-AMD male; *sample 2*, 72-year-old wet AMD female; *sample 3*, 38-year-old non-AMD male; *sample 4*, 71-year-old non-AMD female; *sample 5*, 71-year-old wet AMD female. *Error bars*, S.D.

of the number 7 (bp −3,936 to −3,855 defect) region was 10% higher than that of the number 6 region, and activity of the number 8 (bp −3,936 to −3,789 defect) region was lower than that of the number 7 region (Fig. 4*C*). In addition, the activity of the number 9 (insertion/deletion defect) region was 10–20% lower than that of the number 6 insertion/deletion type transcription regulator (Fig. 4*C*). Taken together, these results suggest that both of the non-insertion/deletion type regions

(including bp −4,320 to −4,239 and bp −3,936 to −3,778 bp) may be regulated by suppressor factors, whereas the insertion/deletion type region from bp −3,836 to −3,789 may bind an enhancer.

Endogenous HTRA1 Expression Is Enhanced by the Insertion/Deletion Type Regulatory Element in AMD Patient iPSCs—To determine the level of *HTRA1* expression in individuals with a non-insertion/deletion type regulatory element sequence,
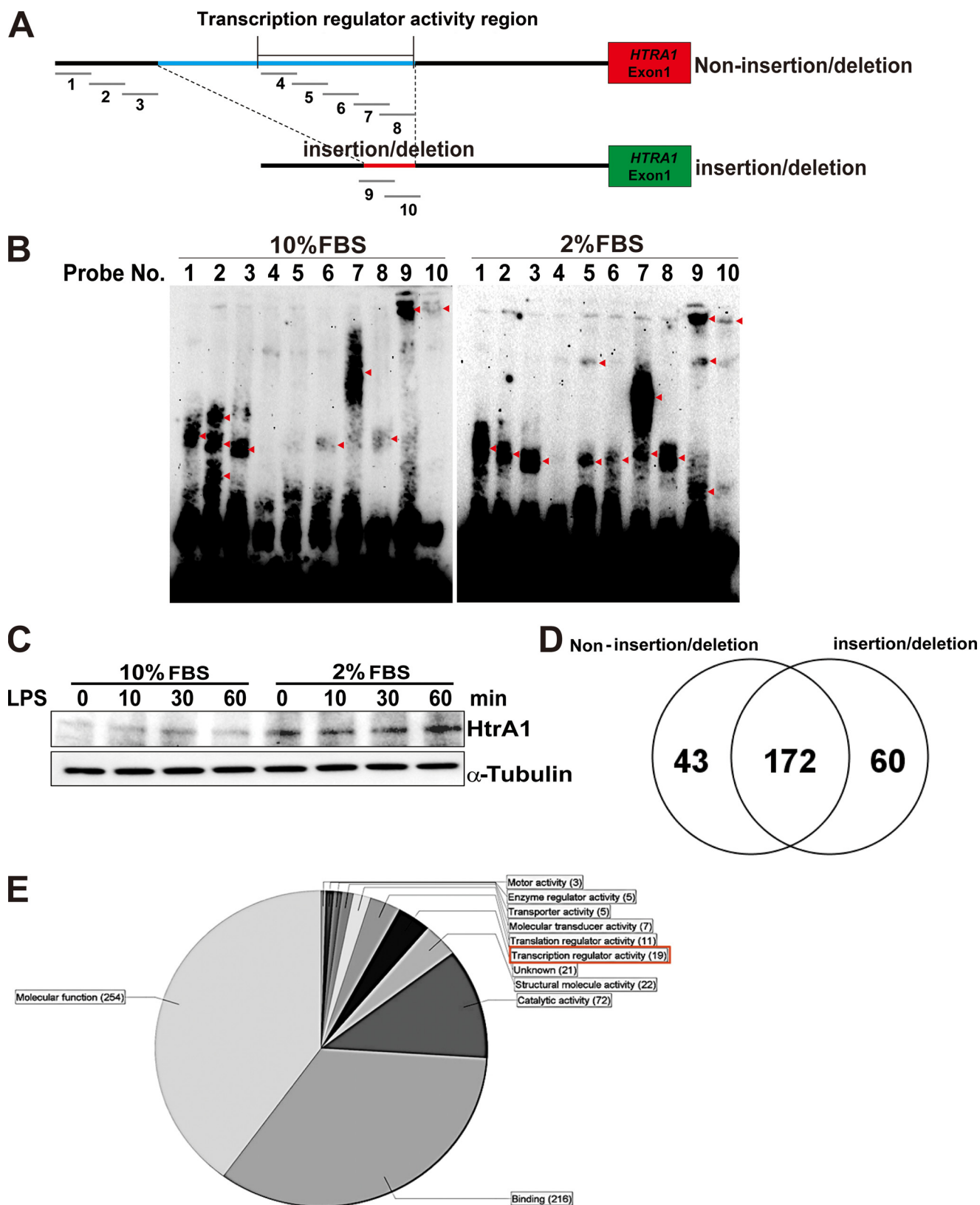
FIGURE 6. **Identification of the transcription factors binding to non-insertion/deletion and insertion/deletion regions of the *HTRA1* transcription regulators.** *A*, location of the double-stranded DNA probes, *1–10*, in the region upstream of the *HTRA1* coding region that were designed for EMSAs. Both non-insertion/deletion and insertion/deletion *HTRA1* transcription regulatory regions were targeted. *B*, EMSAs of probes 1–10 using nuclear extracts from 661W cells cultured in 2 and 10% FBS. *Red arrowheads*, detected signals. *C*, increased expression of HtrA1 was detected in Western blot assays performed following treatment of 661W cells with LPS (1 μg/ml, 0–60 min) using anti-mouse HtrA1 antibodies. Detection of α-tubulin was used as an internal control. *D*, a Venn diagram shows the number of proteins found to bind the non-insertion/deletion *versus* insertion/deletion regions of the *HTRA1* transcription regulator based on LC-MS/MS data. *E*, gene ontology term of non-insertion/deletion- and insertion/deletion-binding protein (categorized by molecular function).

iPSCs heterozygous and homozygous for the insertion/deletion type regulatory element sequence were subjected to genotyping. From both control and AMD patients, iPSCs were collected and categorized as having a non-insertion/deletion or insertion/deletion genotype (Fig. 5A). These cells were also assayed for expression of the iPSCs markers, OCT3/4, NANOG, and SOX2 (Fig. 5B), and levels of *HTRA1* mRNA were measured by RT-PCR and quantitative RT-PCR (Fig. 5, *B* and *C*). Individuals with heterozygous or homozygous *HTRA1* insertion/deletion type sequences showed an approximately 6- and 7-fold increase in *HTRA1* mRNA levels, respectively, compared with individuals having the non-insertion/deletion type sequence (Fig. 5C). In contrast, expression of *HTRA1* mRNA was not influenced by the heterozygous or homozygous state of the insertion/deletion type sequence.

Analysis of Regulatory Element-binding Proteins—To detect proteins that bind the *HTRA1* regulatory element, EMSAs were performed. Ten 3′-biotin-labeled double-stranded DNA probes were generated in order to assay the transcriptional activity of each region of the *HTRA1* regulatory element (Figs. 4 (*B* and *C*) and 6A and Table 3). In addition to the use of 661W nuclear extracts in these assays, extracts of 661W cells grown in 10% FBS *versus* 2% FBS were also assayed; the latter conditions were included based on the observation that HTRA1 family proteins are known to mediate various stress response signaling pathways (25–28). Thus, we tested 661W cell protein-probe binding activity in a cell-stressful environment. Protein-probe binding signals were detected for probes 1–3 and 6–10 (Fig. 6A) in the presence of nuclear extracts from normally cultured 661W cells (Fig. 6B, *left*). These results suggest that the binding pattern of the insertion/deletion sequence (included in probes 4–8) may differ greatly from that of the non-insertion/deletion type sequence (number 9 and 10 probes). When the culturing conditions for the 661W cells were changed from 10% to 2% FBS, this drastically altered the protein-probe binding signal pattern obtained (Fig. 6B, *right*). For example, a reduction in FBS concentration resulted in the loss of two of three signals for the number 2 probe, and it altered the probe-protein binding pattern of probes 5–9. Detection of HtrA1 expression further demonstrated that HtrA1 expression was enhanced in 661W cells following starvation stress (Fig. 6C). Signaling pathways involving the Toll-like receptor (TLR) family of proteins have been shown to be associated with AMD pathogenesis (29), and 661W cells are known to express TLR-4 (30). Therefore, HtrA1 expression was assayed in 661W cells following stimulation with a TLR-4 ligand, lipopolysaccharide (LPS). However, HtrA1 expression was unaffected by this stimulation (Fig. 6C).

To identify the proteins that bind the regulatory element region of *HTRA1*, both non-insertion/deletion and insertion/deletion sequence-binding factors were analyzed by LC-MS/MS. Non-insertion/deletion-binding protein samples were incubated with probes 4–8, whereas the insertion/deletion-binding protein samples were incubated with probes 9 and 10 (Fig. 6A). A total of 172 common binding proteins, 43 non-insertion/deletion probe-specific binding proteins, and 60 insertion/deletion probe-specific binding proteins were identified (Fig. 6D). Using Scaffold 4 software, 19 transcriptional regulator proteins were detected (according to gene ontology (see

the Gene Ontology Consortium Web site)) (Fig. 6E). These 19 factors were then classified according to their binding sequence (Tables 4–6). Six non-insertion/deletion-binding probes were found to bind PURB, NFIC, RUNX2, PEBB, APEX1, and RBM14 proteins (Table 4), whereas three insertion/deletion-binding probes were found to bind LYRIC (lysine-rich CEACAM1 co-isolated) protein, MED4, and PHF2 (Table 5). Ten additional proteins were found to bind both the non-insertion/deletion and insertion/deletion probes: ROAA, SHOX2, CUX1, DDX5, DDX1, MED24, RBM39, JMY, TCP4, and DDX17 (Table 6). In combination, these results suggest that expression of *HtrA1* is influenced by factors that specifically bind this region and affect gene expression.

DISCUSSION

To the best of our knowledge, the present study provides the first detailed characterization of regulatory elements for *HTRA1* and the effect of insertion/deletion sequences associated with wet AMD. The insertion/deletion variant that exhibited complete association with the SNP, rs10490924, is the only major sequence change in this LD block and is likely to play a major role in disease onset. Moreover, the insertion/deletion variant in close proximity to *ARMS2* and *HTRA1* has been at the center of the discussion of whether one or both genes are involved in AMD (19, 24). In the present study, the *ARMS2* transcription regulator exhibited only marginal activity in each of the cell lines tested, whereas robust up-regulation of *HTRA1* transcription regulator activity was observed in iPSCs derived from AMD patients containing heterozygous or homozygous forms of the insertion/deletion. Up-regulation of *HTRA1* in the earliest stages of development is predicted to affect the entire body (31).

HTRA1 is known to be a TGF-β suppression factor, and some reports have suggested that HtrA1 is expressed in skeletal, brain, lung epithelium, heart, and skin tissues in fetal mice (31). Other reports have suggested that HTRA1 is involved in bone remodeling (*e.g.* RANK/RANKL signal-derived osteoclast bone absorption and osteoblast differentiation) (32) and oncogenesis in liver and lung cancers (33, 34). Thus, HTRA1 may play an important role in cell growth and differentiation, tissue and/or organ formation, and the onset of disorders. Correspondingly, a transgenic mouse with expression of mouse *HtrA1* driven by a chicken actin (CAG) promoter was used to establish a model for choroidal neovascularization, and this model exhibited a significant reduction in tolerance to smoking (23).

Detailed characterization of the transcription regulator activity that surrounds the *HTRA1* insertion/deletion sequence showed that suppressive regions are located between bp −4,320 and −4,239 and between bp −3,936 and −3,778 in the non-insertion/deletion sequence and between bp −3,936 and −3,854 for the insertion/deletion sequence. In addition, the insertion/deletion located between bp −3,836 and −3,783 exhibited transcription regulator activity unique to the insertion/deletion sequence (Fig. 4). An analysis of these results showed that the insertion/deletion variant interrupts a suppressor *cis*-element and replaces it with an activator, and this significantly alters *HTRA1* transcription in the photoreceptor.

TABLE 4
Non-insertion/deletion probe binding proteins

MS/MS view: identified proteins	Symbol	Molecular mass	Taxonomy	Biological regulation	Binding	Molecular function	Transcription regulator activity	Peptide hit score (non-indel)[a]	Peptide Hit Score (indel)
		kDa							
Transcriptional activator protein Pur-β	PURB	34	*M. musculus*	Regulation of transcription, DNA-dependent	Protein binding	Transcription factor activity	Transcription factor activity	3	0
Nuclear factor 1 C-type	NFIC	49	*M. musculus*	Regulation of transcription, DNA-dependent	Transcription factor activity	Transcription factor activity	Transcription factor activity	3	0
Runt-related transcription factor 2	RUNX2	66	*M. musculus*	Positive regulation of transcription from RNA polymerase II promoter	Protein binding	Transcription factor activity	Transcription factor activity	2	0
Core-binding factor subunit β	PEBB	22	*M. musculus*	Positive regulation of transcription from RNA polymerase II promoter	DNA binding	Transcription coactivator activity	Transcription coactivator activity	1	0
DNA-(apurinic or apyrimidinic site) lyase	APEX1	35	*M. musculus*	Cell redox homeostasis	Chromatin DNA binding	Transcription coactivator activity	Transcription coactivator activity	1	0
RNA-binding protein 14	RBM14	69	*M. musculus*	Regulation of transcription, DNA-dependent	Nucleic acid binding	Ligand-dependent nuclear receptor transcription coactivator activity	Ligand-dependent nuclear receptor transcription coactivator activity	1	0

[a] indel, insertion/deletion.

TABLE 5
Insertion/deletion probe binding proteins

MS/MS view: identified proteins	Symbol	Molecular mass	Taxonomy	Biological regulation	Binding	Molecular function	Transcription Regulator Activity	Peptide Hit Score (non-indel)[a]	Peptide Hit Score (indel)
		kDa							
Protein LYRIC	LYRIC	64	*M. musculus*	Positive regulation of NF-κB transcription factor activity	Nucleolus	Protein binding	Transcription coactivator activity	0	20
Mediator of RNA polymerase II transcription subunit 4	MED4	30	*M. musculus*	Androgen receptor signaling pathway	Thyroid hormone receptor binding	Transcription cofactor activity	Transcription cofactor activity	0	2
Lysine-specific demethylase PHF2	PHF2	121	*M. musculus*	Regulation of transcription, DNA-dependent	Methylated histone residue binding	Transcription coactivator activity	Transcription coactivator activity	0	1

[a] indel, insertion/deletion.

TABLE 6
Non-insertion/deletion-probe and insertion/deletion probe-binding proteins

MS/MS view: identified proteins	Symbol	Molecular mass (kDa)	Taxonomy	Biological regulation	Binding	Molecular Function	Transcription Regulator Activity	Peptide hit score (non-indel)[a]	Peptide hit score (indel)
Heterogeneous nuclear ribonucleoprotein A/B	HNRPAB	31	*M. musculus*	Regulation of transcription, DNA-dependent	Nucleic acid binding	Transcription factor activity	Transcription factor activity	25	24
Short stature homeobox protein 2	SHOX2	35	*M. musculus*	Positive regulation of transcription from RNA polymerase II promoter	DNA binding	Transcription factor activity	Transcription factor activity	2	1
Homeobox protein cut-like 1	CUX1	166	*M. musculus*	Negative regulation of transcription from RNA polymerase II promoter	Chromatin binding	Transcription factor activity	Transcription factor activity	6	1
Probable ATP-dependent RNA helicase DDX5	DDX5	69	*M. musculus*	Regulation of alternative nuclear mRNA splicing, via spliceosome	Nucleic acid binding	Transcription coactivator activity	Transcription cofactor activity	14	36
ATP-dependent RNA helicase DDX1	DDX1	83	*M. musculus*	Regulation of transcription, DNA-dependent	Chromatin binding	Transcription cofactor activity	Transcription cofactor activity	28	12
Mediator of RNA polymerase II transcription subunit 24	MED24	110	*M. musculus*	Stem cell maintenance	Thyroid hormone receptor binding	Receptor activity	Transcription cofactor activity	1	1
RNA-binding protein 39	RBM39	59	*M. musculus*	Regulation of transcription, DNA-dependent	Nucleic acid binding	Transcription coactivator activity	Transcription coactivator activity	10	9
Junction-mediating and -regulatory protein	JMY	111	*M. musculus*	Positive regulation of transcription factor activity	Protein binding	Transcription coactivator activity	Transcription coactivator activity	1	1
Activated RNA polymerase II transcriptional coactivator p15	TCP4	14	*M. musculus*	Regulation of transcription from RNA polymerase II promoter	DNA binding	Transcription coactivator activity	Transcription coactivator activity	1	2
Probable ATP-dependent RNA helicase DDX17	DDX17	72	*M. musculus*	Regulation of transcription, DNA-dependent	Nucleic acid binding	Hydrolase activity	Transcription coactivator activity	1	1

[a] indel, insertion/deletion.

The EMSA and LC-MS/MS data also suggest that *HTRA1* regulatory element activity is regulated by a number of transcription factors (Fig. 6 and Tables 4–6).

When the proteins that bound the regulatory elements of the non-insertion/deletion and insertion/deletion sequences of *HTRA1* were analyzed using LC-MS/MS, LYRIC (also known as MTDH/AEG1) was a high hit score insertion/deletion-binding protein that was identified (Table 5). LYRIC is known to promote hepatocellular carcinoma and to activate the transcription factor, nuclear factor κ-B (NF-κB), and also has an effect on bone and brain metastasis (35–37). Regarding the latter, LYRIC may enhance the seeding of tumor cells at the target organ endothelium. LYRIC also contributes to HIF-1α-mediated angiogenesis (38), with HIF-1α playing an important role in the activation of VEGF signaling in response to oxidative stress (39). Recently, Oka *et al.* (25) reported that *HTRA1* gene expression is enhanced by oxidative stress. This result is consistent with the observation that AMD onset is associated with a variety of stresses, and stress response factors may play an important role.

Both common sequences (non-insertion/deletion (bp −4,320 to −4,220) and insertion/deletion (bp −3,936 to −3,836 bp)) and the insertion/deletion sequence (bp −3,836 to −3,782 bp) are partially associated with *ARMS2* exon 2, thereby indicating that this exon represents a protein-coding region and a *HTRA1* regulatory element region. Recent reports have suggested that both an increase in HTRA1 transcription and a decrease in ARMS2 transcription confer an increased risk of AMD (8). These insights suggest that *ARMS2* gene expression may be regulated by *HTRA1* transcription regulator activity via the *ARMS2* exon 2 region.

AMD pathogenesis and previous *HTRA1* experiments related to AMD have been performed and discussed in relation to the RPE (8, 16, 17). However, immunostaining of *HTRA1* in mouse retinas in the present study showed that the majority of transcription occurs in the photoreceptor cell layer (Fig. 3). This result was confirmed when higher levels of transcription from the *HTRA1* insertion/deletion regulator were observed in the photoreceptor cell line: 661W cells *versus* the RPE cells (Fig. 1, *I–K*). Photoreceptors are densely concentrated in the macula (40), which predicts that HTRA1 will also be concentrated in the macula. A recent report using transgenic mice overexpressing human HTRA1 in the RPE showed that PCV-like capillary structures could be observed in the choroid. Vierkotten *et al.* (17) also observed fragmentation of the elastic layer in Bruch's membrane, and Jones *et al.* (16) reported branching of choroidal vessels, polypoidal lesions, and severe degeneration of the elastic lamina or tunica media of choroidal vessels in the same model. When *HtrA1* expression was driven by the CAG promoter in a transgenic mouse model, an even more severe phenotype was induced compared with previous reports of AMD patient-like choroidal neovascularization (23). These results indicate that overexpression of HtrA1 alone can evoke choroidal vasculopathy or neovascularization, and they also provide supporting evidence for the association of the insertion/deletion variant of *HTRA1* regulatory element with wet AMD (7, 8).

REFERENCES

1. Fritsche, L. G., Chen, W., Schu, M., Yaspan, B. L., Yu, Y., Thorleifsson, G., Zack, D. J., Arakawa, S., Cipriani, V., Ripke, S., Igo, R. P., Jr., Buitendijk, G. H., Sim, X., Weeks, D. E., Guymer, R. H., Merriam, J. E., Francis, P. J., Hannum, G., Agarwal, A., Armbrecht, A. M., Audo, I., Aung, T., Barile, G. R., Benchaboune, M., Bird, A. C., Bishop, P. N., Branham, K. E., Brooks, M., Brucker, A. J., Cade, W. H., Cain, M. S., Campochiaro, P. A., Chan, C. C., Cheng, C. Y., Chew, E. Y., Chin, K. A., Chowers, I., Clayton, D. G., Cojocaru, R., Conley, Y. P., Cornes, B. K., Daly, M. J., Dhillon, B., Edwards, A. O., Evangelou, E., Fagerness, J., Ferreyra, H. A., Friedman, J. S., Geirsdottir, A., George, R. J., Gieger, C., Gupta, N., Hagstrom, S. A., Harding, S. P., Haritoglou, C., Heckenlively, J. R., Holz, F. G., Hughes, G., Ioannidis, J. P., Ishibashi, T., Joseph, P., Jun, G., Kamatani, Y., Katsanis, N., C, N. K., Khan, J. C., Kim, I. K., Kiyohara, Y., Klein, B. E., Klein, R., Kovach, J. L., Kozak, I., Lee, C. J., Lee, K. E., Lichtner, P., Lotery, A. J., Meitinger, T., Mitchell, P., Mohand-Said, S., Moore, A. T., Morgan, D. J., Morrison, M. A., Myers, C. E., Naj, A. C., Nakamura, Y., Okada, Y., Orlin, A., Ortube, M. C., Othman, M. I., Pappas, C., Park, K. H., Pauer, G. J., Peachey, N. S., Poch, O., Priya, R. R., Reynolds, R., Richardson, A. J., Ripp, R., Rudolph, G., Ryu, E., Sahel, J. A., Schaumberg, D. A., Scholl, H. P., Schwartz, S. G., Scott, W. K., Shahid, H., Sigurdsson, H., Silvestri, G., Sivakumaran, T. A., Smith, R. T., Sobrin, L., Souied, E. H., Stambolian, D. E., Stefansson, H., Sturgill-Short, G. M., Takahashi, A., Tosakulwong, N., Truitt, B. J., Tsironi, E. E., Uitterlinden, A. G., van Duijn, C. M., Vijaya, L., Vingerling, J. R., Vithana, E. N., Webster, A. R., Wichmann, H. E., Winkler, T. W., Wong, T. Y., Wright, A. F., Zelenika, D., Zhang, M., Zhao, L., Zhang, K., Klein, M. L., Hageman, G. S., Lathrop, G. M., Stefansson, K., Allikmets, R., Baird, P. N., Gorin, M. B., Wang, J. J., Klaver, C. C., Seddon, J. M., Pericak-Vance, M. A., Iyengar, S. K., Yates, J. R., Swaroop, A., Weber, B. H., Kubo, M., Deangelis, M. M., Leveillard, T., Thorsteinsdottir, U., Haines, J. L., Farrer, L. A., Heid, I. M., and Abecasis, G. R. (2013) Seven new loci associated with age-related macular degeneration. *Nat. Genet.* 10.1038/ng.2578

2. Klein, R. J., Zeiss, C., Chew, E. Y., Tsai, J. Y., Sackler, R. S., Haynes, C., Henning, A. K., SanGiovanni, J. P., Mane, S. M., Mayne, S. T., Bracken, M. B., Ferris, F. L., Ott, J., Barnstable, C., and Hoh, J. (2005) Complement factor H polymorphism in age-related macular degeneration. *Science* **308,** 385–389

3. Hageman, G. S., Anderson, D. H., Johnson, L. V., Hancox, L. S., Taiber, A. J., Hardisty, L. I., Hageman, J. L., Stockman, H. A., Borchardt, J. D., Gehrs, K. M., Smith, R. J., Silvestri, G., Russell, S. R., Klaver, C. C., Barbazetto, I., Chang, S., Yannuzzi, L. A., Barile, G. R., Merriam, J. C., Smith, R. T., Olsh, A. K., Bergeron, J., Zernant, J., Merriam, J. E., Gold, B., Dean, M., and Allikmets, R. (2005) A common haplotype in the complement regulatory gene factor H (HF1/CFH) predisposes individuals to age-related macular degeneration. *Proc. Natl. Acad. Sci. U.S.A.* **102,** 7227–7232

4. Okamoto, H., Umeda, S., Obazawa, M., Minami, M., Noda, T., Mizota, A., Honda, M., Tanaka, M., Koyama, R., Takagi, I., Sakamoto, Y., Saito, Y., Miyake, Y., and Iwata, T. (2006) Complement factor H polymorphisms in Japanese population with age-related macular degeneration. *Mol. Vis.* **12,** 156–158

5. Kondo, N., Honda, S., Ishibashi, K., Tsukahara, Y., and Negi, A. (2007) LOC387715/HTRA1 variants in polypoidal choroidal vasculopathy and age-related macular degeneration in a Japanese population. *Am. J. Ophthalmol.* **144,** 608–612

6. Goto, A., Akahori, M., Okamoto, H., Minami, M., Terauchi, N., Haruhata, Y., Obazawa, M., Noda, T., Honda, M., Mizota, A., Tanaka, M., Hayashi, T., Tanito, M., Ogata, N., and Iwata, T. (2009) Genetic analysis of typical wet-type age-related macular degeneration and polypoidal choroidal vasculopathy in Japanese population. *J. Ocul. Biol. Dis. Infor.* **2,** 164–175

7. Fritsche, L. G., Loenhardt, T., Janssen, A., Fisher, S. A., Rivera, A., Keilhauer, C. N., and Weber, B. H. (2008) Age-related macular degeneration is associated with an unstable ARMS2 (LOC387715) mRNA. *Nat. Genet.* **40,** 892–896

8. Yang, Z., Tong, Z., Chen, Y., Zeng, J., Lu, F., Sun, X., Zhao, C., Wang, K., Davey, L., Chen, H., London, N., Muramatsu, D., Salasar, F., Carmona, R., Kasuga, D., Wang, X., Bedell, M., Dixie, M., Zhao, P., Yang, R., Gibbs, D., Liu, X., Li, Y., Li, C., Li, Y., Campochiaro, B., Constantine, R., Zack, D. J., Campochiaro, P., Fu, Y., Li, D. Y., Katsanis, N., and Zhang, K. (2010) Genetic and functional dissection of HTRA1 and LOC387715 in age-related macular degeneration. *PLoS Genet.* **6,** e1000836

9. Kanda, A., Chen, W., Othman, M., Branham, K. E., Brooks, M., Khanna, R., He, S., Lyons, R., Abecasis, G. R., and Swaroop, A. (2007) A variant of mitochondrial protein LOC387715/ARMS2, not HTRA1, is strongly associated with age-related macular degeneration. *Proc. Natl. Acad. Sci. U.S.A.* **104,** 16227–16232

10. Kortvely, E., Hauck, S. M., Duetsch, G., Gloeckner, C. J., Kremmer, E., Alge-Priglinger, C. S., Deeg, C. A., and Ueffing, M. (2010) ARMS2 is a constituent of the extracellular matrix providing a link between familial and sporadic age-related macular degenerations. *Invest. Ophthalmol. Vis. Sci.* **51,** 79–88

11. Shiga, A., Nozaki, H., Yokoseki, A., Nihonmatsu, M., Kawata, H., Kato, T., Koyama, A., Arima, K., Ikeda, M., Katada, S., Toyoshima, Y., Takahashi, H., Tanaka, A., Nakano, I., Ikeuchi, T., Nishizawa, M., and Onodera, O. (2011) Cerebral small-vessel disease protein HTRA1 controls the amount of TGF-β1 via cleavage of proTGF-β1. *Hum. Mol. Genet.* **20,** 1800–1810

12. Zhang, L., Lim, S. L., Du, H., Zhang, M., Kozak, I., Hannum, G., Wang, X., Ouyang, H., Hughes, G., Zhao, L., Zhu, X., Lee, C., Su, Z., Zhou, X., Shaw, R., Geum, D., Wei, X., Zhu, J., Ideker, T., Oka, C., Wang, N., Yang, Z., Shaw, P. X., and Zhang, K. (2012) High temperature requirement factor A1 (HTRA1) gene regulates angiogenesis through transforming growth factor-β family member growth differentiation factor 6. *J. Biol. Chem.* **287,** 1520–1526

13. Jiang, J., Huang, L., Yu, W., Wu, X., Zhou, P., and Li, X. (2012) Overexpression of HTRA1 leads to down-regulation of fibronectin and functional changes in RF/6A cells and HUVECs. *PLoS One* **7,** e46115

14. Ferrer-Vaquer, A., Maurey, P., Werzowa, J., Firnberg, N., Leibbrandt, A., and Neubüser, A. (2008) Expression and regulation of HTRA1 during chick and early mouse development. *Dev. Dyn.* **237,** 1893–1900

15. Chien, J., Ota, T., Aletti, G., Shridhar, R., Boccellino, M., Quagliuolo, L., Baldi, A., and Shridhar, V. (2009) Serine protease HtrA1 associates with microtubules and inhibits cell migration. *Mol. Cell. Biol.* **29,** 4177–4187

16. Jones, A., Kumar, S., Zhang, N., Tong, Z., Yang, J. H., Watt, C., Anderson, J., Amrita, Fillerup, H., McCloskey, M., Luo, L., Yang, Z., Ambati, B., Marc, R., Oka, C., Zhang, K., and Fu, Y. (2011) Increased expression of multifunctional serine protease, HTRA1, in retinal pigment epithelium induces polypoidal choroidal vasculopathy in mice. *Proc. Natl. Acad. Sci. U.S.A.* **108,** 14578–14583

17. Vierkotten, S., Muether, P. S., and Fauser, S. (2011) Overexpression of HTRA1 leads to ultrastructural changes in the elastic layer of Bruch's membrane via cleavage of extracellular matrix components. *PLoS One* **6,** e22959

18. Hara, K., Shiga, A., Fukutake, T., Nozaki, H., Miyashita, A., Yokoseki, A., Kawata, H., Koyama, A., Arima, K., Takahashi, T., Ikeda, M., Shiota, H., Tamura, M., Shimoe, Y., Hirayama, M., Arisato, T., Yanagawa, S., Tanaka, A., Nakano, I., Ikeda, S., Yoshida, Y., Yamamoto, T., Ikeuchi, T., Kuwano, R., Nishizawa, M., Tsuji, S., and Onodera, O. (2009) Association of HTRA1 mutations and familial ischemic cerebral small-vessel disease. *N. Engl. J. Med.* **360,** 1729–1739

19. Dewan, A., Liu, M., Hartman, S., Zhang, S. S., Liu, D. T., Zhao, C., Tam, P. O., Chan, W. M., Lam, D. S., Snyder, M., Barnstable, C., Pang, C. P., and Hoh, J. (2006) HTRA1 promoter polymorphism in wet age-related macular degeneration. *Science* **314,** 989–992

20. Seddon, J. M., Ajani, U. A., and Mitchell, B. D. (1997) Familial aggregation of age-related maculopathy. *Am. J. Ophthalmol.* **123,** 199–206

21. Seki, T., Yuasa, S., Oda, M., Egashira, T., Yae, K., Kusumoto, D., Nakata, H., Tohyama, S., Hashimoto, H., Kodaira, M., Okada, Y., Seimiya, H., Fusaki, N., Hasegawa, M., and Fukuda, K. (2010) Generation of induced pluripotent stem cells from human terminally differentiated circulating T cells. *Cell Stem Cell* **7,** 11–14

22. Minegishi, Y., Iejima, D., Kobayashi, H., Chi, Z. L., Kawase, K., Yamamoto, T., Seki, T., Yuasa, S., Fukuda, K., and Iwata, T. (2013) Enhanced optineurin E50K-TBK1 interaction evokes protein insolubility and initiates familial primary open-angle glaucoma. *Hum. Mol. Genet.* **22,** 3559–3567

23. Nakayama, M., Iejima, D., Akahori, M., Kamei, J., Goto, A., and Iwata, T. (2014) Overexpression of HtrA1 and exposure to mainstream cigarette

smoke leads to choroidal neovascularization and subretinal deposits in aged mice. *Invest. Ophthalmol. Vis. Sci.* **55,** 6514–6523

24. Yang, Z., Camp, N. J., Sun, H., Tong, Z., Gibbs, D., Cameron, D. J., Chen, H., Zhao, Y., Pearson, E., Li, X., Chien, J., Dewan, A., Harmon, J., Bernstein, P. S., Shridhar, V., Zabriskie, N. A., Hoh, J., Howes, K., and Zhang, K. (2006) A variant of the HTRA1 gene increases susceptibility to age-related macular degeneration. *Science* **314,** 992–993

25. Supanji, Shimomachi, M., Hasan, M. Z., Kawaichi, M., and Oka, C. (2013) HtrA1 is induced by oxidative stress and enhances cell senescence through p38 MAPK pathway. *Exp. Eye Res.* **112,** 79–92

26. Hansen, G., and Hilgenfeld, R. (2013) Architecture and regulation of HtrA-family proteins involved in protein quality control and stress response. *Cell Mol. Life Sci.* **70,** 761–775

27. Gray, C. W., Ward, R. V., Karran, E., Turconi, S., Rowles, A., Viglienghi, D., Southan, C., Barton, A., Fantom, K. G., West, A., Savopoulos, J., Hassan, N. J., Clinkenbeard, H., Hanning, C., Amegadzie, B., Davis, J. B., Dingwall, C., Livi, G. P., and Creasy, C. L. (2000) Characterization of human HtrA2, a novel serine protease involved in the mammalian cellular stress response. *Eur. J. Biochem.* **267,** 5699–5710

28. Foucaud-Scheunemann, C., and Poquet, I. (2003) HtrA is a key factor in the response to specific stress conditions in *Lactococcus lactis*. *FEMS Microbiol. Lett.* **224,** 53–59

29. Kleinman, M. E., Kaneko, H., Cho, W. G., Dridi, S., Fowler, B. J., Blandford, A. D., Albuquerque, R. J., Hirano, Y., Terasaki, H., Kondo, M., Fujita, T., Ambati, B. K., Tarallo, V., Gelfand, B. D., Bogdanovich, S., Baffi, J. Z., and Ambati, J. (2012) Short-interfering RNAs induce retinal degeneration via TLR3 and IRF3. *Mol. Ther.* **20,** 101–108

30. Tu, Z., Portillo, J. A., Howell, S., Bu, H., Subauste, C. S., Al-Ubaidi, M. R., Pearlman, E., and Lin, F. (2011) Photoreceptor cells constitutively express functional TLR4. *J. Neuroimmunol.* **230,** 183–187

31. Oka, C., Tsujimoto, R., Kajikawa, M., Koshiba-Takeuchi, K., Ina, J., Yano, M., Tsuchiya, A., Ueta, Y., Soma, A., Kanda, H., Matsumoto, M., and Kawaichi, M. (2004) HtrA1 serine protease inhibits signaling mediated by Tgfβ family proteins. *Development* **131,** 1041–1053

32. Wu, X., Chim, S. M., Kuek, V., Lim, B. S., Chow, S. T., Zhao, J., Yang, S., Rosen, V., Tickner, J., and Xu, J. (2014) HtrA1 is upregulated during RANKL-induced osteoclastogenesis, and negatively regulates osteoblast differentiation and BMP2-induced Smad1/5/8, ERK and p38 phosphorylation. *FEBS Lett.* **588,** 143–150

33. Zhu, F., Jin, L., Luo, T. P., Luo, G. H., Tan, Y., and Qin, X. H. (2010) Serine protease HtrA1 expression in human hepatocellular carcinoma. *Hepatobiliary Pancreat. Dis. Int.* **9,** 508–512

34. Xu, Y., Jiang, Z., Zhang, Z., Sun, N., Zhang, M., Xie, J., Li, T., Hou, Y., and Wu, D. (2013) HtrA1 downregulation induces cisplatin resistance in lung adenocarcinoma by promoting cancer stem cell-like properties. *J. Cell. Biochem.* **115,** 1112–1121

35. Ash, S. C., Yang, D. Q., and Britt, D. E. (2008) LYRIC/AEG-1 overexpression modulates BCCIPα protein levels in prostate tumor cells. *Biochem. Biophys. Res. Commun.* **371,** 333–338

36. Robertson, C. L., Srivastava, J., Siddiq, A., Gredler, R., Emdad, L., Rajasekaran, D., Akiel, M., Shen, X. N., Guo, C., Giashuddin, S., Wang, X. Y., Ghosh, S., Subler, M. A., Windle, J. J., Fisher, P. B., and Sarkar, D. (2014) Genetic deletion of AEG-1 prevents hepatocarcinogenesis. *Cancer Res.* **74,** 6184–6193

37. Huang, Y., and Li, L. P. (2014) Progress of cancer research on astrocyte elevated gene-1/metadherin (review). *Oncol. Lett.* **8,** 493–501

38. Noch, E., Bookland, M., and Khalili, K. (2011) Astrocyte-elevated gene-1 (AEG-1) induction by hypoxia and glucose deprivation in glioblastoma. *Cancer Biol. Ther.* **11,** 32–39

39. Domigan, C. K., and Iruela-Arispe, M. L. (2014) Stealing VEGF from thy neighbor. *Cell* **159,** 473–474

40. Li, K. Y., Tiruveedhula, P., and Roorda, A. (2010) Intersubject variability of foveal cone photoreceptor density in relation to eye length. *Invest. Ophthalmol. Vis. Sci.* **51,** 6858–6867